

On the kinematic constraint in BFKL near threshold region

Hao-yu Liu,¹ Xiao-hui Liu,¹ Yu Shi,² Du-xin Zheng,³ and Jian Zhou²

¹*Center of Advanced Quantum Studies, Department of Physics,
Beijing Normal University, Beijing, China*

²*Key Laboratory of Particle Physics and Particle Irradiation (MOE),
Institute of Frontier and Interdisciplinary Science,
Shandong University, QingDao, China*

³*School of Physics and State Key Laboratory of Nuclear
Physics and Technology, Peking University, Beijing, China*

Abstract

We introduce a modified Balitskii-Fadin-Kuraev-Lipatov (BFKL) equation with the rapidity veto that originates from external kinematic constraint. Though it is a formally sub-leading power contribution, such kinematic effect becomes very important especially in the threshold region, where there is no sufficient phase space for the small x evolution to be fully developed. We also investigate the phenomenological consequences of the kinematic constraint BFKL equation in the forward particle production processes in pp and eA collisions. It is shown that particle yield at large transverse momentum is significantly suppressed in the threshold region.

I. INTRODUCTION

Understanding the behavior of parton densities at small x is one of the important aspects of the nucleon/nucleus internal structure studies. It is also crucial for describing the experimental data of high energy scattering processes in ep/eA and pp/pA collisions. The small x evolution of the unintegrated gluon distribution is governed by the famous BFKL equation [1, 2] in the dilute limit. When the parton density is so high that the gluon fusion process becomes important, the proper evolution equation for describing small x dynamics is the JIMWLK equation [3–6] or its large N_c version: the BK equation [7, 8]. To improve the precision of the BFKL/BK predication for phenomenology, it is necessary to carry out the program for computing the next-to-leading-order (NLO) corrections to the small x evolution equations, which has been achieved in the recent years [9–12]. Another major development along the direction is the establishment of the joint small x and k_\perp resummation formalism [13–17]. On the other hand, the calculations of the impact factors in various high energy scattering processes have been pushed to the NLO level as well [18–32].

A known issue with the NLO BFKL or BK equations is that the next-to-leading logarithmic (NLL) contribution are large compared to the leading $\log \ln \frac{1}{x}$, which renders the result unstable. These sub-leading logs thus need to be resummed to all orders. One way of including part of the NLL contributions is to enforce the kinematic constraint in the small x evolution equations [33–38]. The implementation of the kinematic constraint was motivated by the requirement that the off-shellness of the exchanged gluon in the BFKL cascade are dominated by the transverse components. Though such kinematic corrections formally are the next-to-leading logarithmic contribution, they are shown to be numerically very large as compared to the leading log result. It thus has long been recognized as the necessary ingredients for the phenomenological application of small x resummation formalism [37, 39]. Other elaborated resummation schemes can be found in Refs. [40–44].

In this work, we introduce a novel NLL BFKL equation that originates from the external kinematic constraint. The key observation that motivates this modified BFKL equation is that the minimal longitudinal momentum fraction of the radiated gluon Δx is finite. The minimal Δx is determined by the onshell condition $\Delta x P^+ > \frac{l_\perp^2}{2P_{\max}^-}$ where l_\perp is the radiated gluon's transverse momentum and P_{\max}^- is the largest possible minus component of longitudinal momentum transferred from the projectile. By imposing this kinematic constraint, the resulting small x log is $\int_{x_g+\Delta x}^1 \frac{dx}{x} = \ln \frac{1}{x_g+\Delta x}$ instead of the conventional one $\ln \frac{1}{x_g}$. Obviously, such kinematic constraint BFKL will slow down small x evolution as compared to the standard BFKL. And in particular, this effect is greatly enhanced in the threshold region where the available P_{\max}^- is very small. The main goal of the paper is to numerically solve the kinematic constraint BFKL equation, and investigate its impact on the phenomenology studies.

The paper is structured as follows. In Sec.II, we first discuss the BFKL equation with kinematic constraint and present numerical solutions. In Sec.III, we study the inclusive forward hadron production in pp collisions by applying the kinematic constraint BFKL evolution. It is shown that subtracting the NLL BFKL instead of the leading log BFKL from the hard part leads to a more stable NLO result. We also make predictions for forward jet production in the small x limit in SIDIS process. It is found that transverse momentum spectrum of the cross section is suppressed due to the limited phase space available for real radiations near threshold region. The paper is summarized in Sec. IV.

II. THE BFKL EQUATION WITH EXTERNAL KINEMATIC CONSTRAINT

We start the discussion about the kinematic constraint BFKL with an explicit example: inclusive forward particle production in pp collisions. The leading order calculation of this process is formulated in a hybrid approach where the projectile is described by the normal parton distribution function(PDF), while the target is treated in the small x formalism [45]. If the outgoing parton carries longitudinal momentum $x_p P^-$, the maximal minus component of the exchanged gluon's momentum is $(1 - x_p)P^-$ according to the four momentum conservation. When x_p approaches 1, the small x evolution is hampered due to the limited phase space for the real correction to the BFKL kernel, particularly at high transverse momentum. Note that such kinematic constraint is different from the one studied in the literature [33–37].

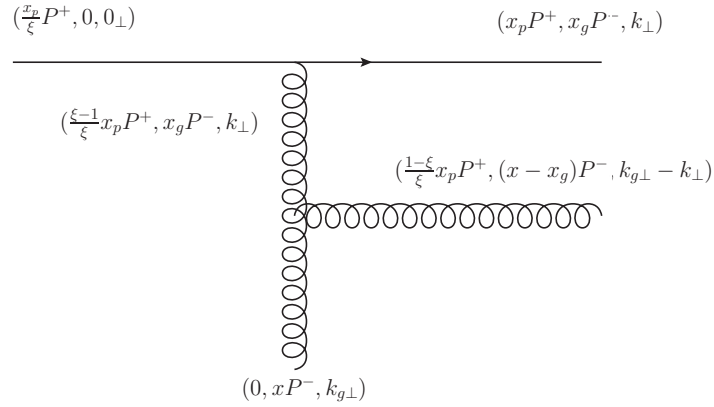


FIG. 1: A real diagram representing gluon emission in the BFKL chain in the forward particle production from quark channel in pp collisions. The incident quark moves along z direction, while the target moves in the opposite direction. The light-cone momenta variables are commonly defined.

We now explain how to implement this new type kinematical constraint in the BFKL evolution. In the leading logarithmic approximation, the standard BFKL equation for the unpolarized gluon TMD (often referred to as the unintegrated gluon distribution as well) reads,

$$G(x_g, k_\perp) = G_0(x_g, k_\perp) + \frac{\alpha_s N_c}{\pi^2} \int_{x_g}^1 \frac{dx}{x} \int d^2 k_{g\perp} \left\{ \frac{G(x, k_{g\perp})}{(k_\perp - k_{g\perp})^2} - \frac{k_\perp^2 G(x, k_\perp)}{(k_\perp - k_{g\perp})^2 [k_{g\perp}^2 + (k_\perp - k_{g\perp})^2]} \right\} \quad (1)$$

where $G_0(x_g, k_\perp)$ is the bare gluon TMD. k_\perp and $k_\perp - k_{g\perp}$ are the transverse momenta of the exchanged gluon and the emitted gluon respectively. The flow of the momenta in the BFKL cascade is illustrated in Fig. 1. To isolate the leading log contribution in the each rung of the BFKL ladder diagram, the virtuality of the exchanged gluon is required to be

$$|2 \frac{\xi - 1}{\xi} x_g x_p P^+ P^- - k_\perp^2| \sim k_\perp^2 \quad (2)$$

This subsequently converts to the condition,

$$2 \frac{1 - \xi}{\xi} x_g x_p P^+ P^- < c k_\perp^2 \quad (3)$$

where we set the coefficient c to be 1 for simplicity. The on-shell condition for the emitted gluon yields,

$$2\frac{1-\xi}{\xi}(x-x_g)x_pP^+P^- = (k_{g\perp} - k_\perp)^2 \quad (4)$$

Moreover, the strong ordering of the longitudinal momenta in the BFKL kinematics implies,

$$x_g \ll x \quad (5)$$

Replacing $x - x_g$ with x in Eq. (4) and inserting it into Eq. (3), one obtains,

$$(k_{g\perp} - k_\perp)^2 < \frac{x}{x_g} k_\perp^2 \quad (6)$$

which imposes an upper limit for the transverse momentum phase space integration that is unconstrained in the standard BFKL equation. Such kinematic constraint and various different approximate forms have been extensively studied in the past [33–37]. Other NLL contributions to in the small x limit were discussed in Refs. [15–17, 40, 42, 46–48].

On the other hand, one can derive a different cutoff for phase space integration by taking into account the constraint from external kinematics. From Eq.(4), one has,

$$x = x_g + \frac{(k_{g\perp} - k_\perp)^2}{2x_pP^+P^-} \frac{\xi}{1-\xi} > x_g + \frac{(k_{g\perp} - k_\perp)^2}{2(1-x_p)P^+P^-} \quad (7)$$

due to $\xi > x_p$. The lower limit for longitudinal momentum integration for real correction in Eq. (2) has to be correspondingly modified as,

$$\int_{x_g}^1 \frac{dx}{x} \longrightarrow \int_{x_g+\Delta x}^1 \frac{dx}{x} \quad (8)$$

where $\Delta x = \frac{(k_\perp - k_{g\perp})^2}{(1-x_p)s}$ is the minimal longitudinal momentum fraction carried by the emitted gluon. This simple analysis obviously can be applied to the gluon emission from each rung of the BFKL ladder because the largest plus momentum component acquired by each emitted gluon must be smaller than $(1-x_p)P^+$. Such kinematic constraint naturally leads to a BFKL equation with a rapidity veto,

$$G(x_g, k_\perp) = G_0(x_g, k_\perp) + \frac{\alpha_s N_c}{\pi^2} \int d^2 k_{g\perp} \left\{ \int_{x_g+\Delta x}^1 \frac{dx}{x} \frac{G(x, k_{g\perp})}{(k_\perp - k_{g\perp})^2} - \int_{x_g}^1 dx \frac{k_\perp^2 G(x, k_\perp)}{x (k_\perp - k_{g\perp})^2 [k_{g\perp}^2 + (k_\perp - k_{g\perp})^2]} \right\} \quad (9)$$

Note that the virtual correction is not affected by the kinematic effect under consideration, and thus remains unchanged. We now compare this new type kinematic constraint with the one that is extensively discussed in literature. To this end, we re-express the on-shell condition in the strong rapidity ordering region as,

$$(k_{g\perp} - k_\perp)^2 = \frac{1-\xi}{\xi} \frac{x-x_g}{x_g} k_\perp^2 < \frac{1-x_p}{x_p} \frac{x}{x_g} k_\perp^2 \quad (10)$$

It is easy to see that at least in the last step of the evolution, this is a more stringent condition than that given by Eq. (6) in the threshold region $x_p \rightarrow 1$, which is the main focus of the present work. Therefore, we will not impose the kinematic constraint Eq. (6), but only modify the lower limit of x integration for real correction part of the BFKL kernel as shown in Eq. (9).

Due to the limited available phase space for real gluon emissions, the small x evolution can not fully develop as described by the standard LL BFKL equation. One may anticipate that the kinematic constraint will significantly slow down the small x evolution, in particular, at large transverse momentum near threshold region. To investigate the impact of the NLL contribution from the kinematic constraint numerically, we derive the differential form of the BFKL equation, which can be straightforwardly obtained by differentiating in $\ln \frac{1}{x_g}$ on both sides of Eq. (9),

$$\begin{aligned} \frac{\partial G(x_g, k_\perp)}{\partial \ln \frac{1}{x_g}} &= \frac{\partial G_0(x_g, k_\perp)}{\partial \ln 1/x_g} \\ &+ \frac{\alpha_s N_c}{\pi^2} \int d^2 k_{g\perp} \left\{ \frac{x_g}{x_g + \Delta x} \frac{G(x_g + \Delta x, k_{g\perp})}{(k_\perp - k_{g\perp})^2} - \frac{k_\perp^2 G(x_g, k_\perp)}{(k_\perp - k_{g\perp})^2 [k_{g\perp}^2 + (k_\perp - k_{g\perp})^2]} \right\} \end{aligned} \quad (11)$$

We use the MV model as the initial condition for the unevolved gluon TMD,

$$G_0(x_g, k_\perp) = \frac{k_\perp^2 N_c}{2\pi^2 \alpha_s} S_\perp \int \frac{d^2 r_\perp}{(2\pi)^2} e^{-ik_\perp \cdot r_\perp} \exp \left[-\frac{r_\perp^2 Q_{s0}^2}{4} \ln \left(\frac{1}{r_\perp \Lambda_{\text{mv}}} + e \right) \right] \quad (12)$$

where $S_\perp = 51\text{mb}$ denotes the transverse area of the proton target, $Q_{s0}^2 = 0.5 \text{ GeV}^2$ is the saturation scale at $x_0 = 0.01$. $\Lambda_{\text{mv}} = 0.241 \text{ GeV}$ is the infrared cutoff in the MV model. It is well known that the leading order BFKL gives a much too steep growth with $1/x$. This is to some extent related to the infrared diffusion of the BFKL dynamics, to avoid which, we numerically solve the kinematic constraint BFKL by imposing a saturation boundary, namely, $\frac{\alpha_s(k_\perp)G(x_g, k_\perp)}{k_\perp^2} = \frac{\alpha_s(k_\perp)G(x_g, k_\perp)}{k_\perp^2} \Big|_{k_\perp=0.7 \text{ GeV}}$ when $k_\perp < 0.7 \text{ GeV}$. Such phenomenological treatment for regularizing the infrared behavior is similar to that proposed in Ref. [49].

In the practical numerical implementations of the kinematic constraint BFKL evolution, we used the running coupling prescription taken from Ref. [50]. The numerical results as a function of the k_\perp for a given Δx are shown in Fig. 2. As a comparison, the solution of the standard running coupling BFKL without kinematic constraint are also presented. It is clear that the solution of the BFKL equation with a rapidity veto constraint gets suppressed at large transverse momentum.

III. PHENOMENOLOGY

In this section, we investigate the impact of the kinematic constraint BFKL evolution on the phenomenology studies in two processes: inclusive forward particle production in pp collisions and forward jet production in SIDIS processes. When the measured particle/jet carries the most longitudinal momentum fraction of the projectile, there is no much phase space left for the radiated gluons to drive the small x evolution. We shall observe that the particle/jet yield is suppressed at relatively large transverse momentum due to the incomplete cancellation between the real and virtual corrections near threshold region.

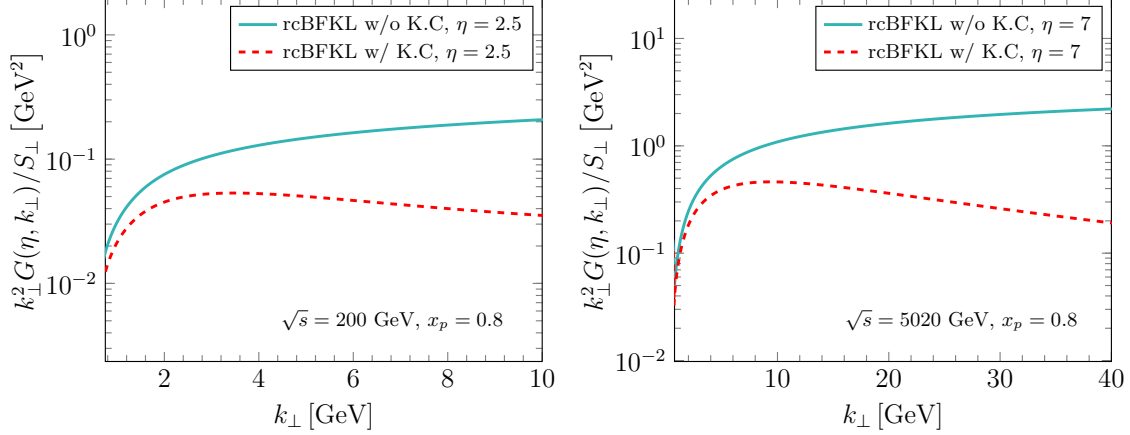


FIG. 2: The comparisons of gluon TMDs with and without the kinematic constraint at RHIC and LHC energies with $\Delta x = \frac{(k_\perp - k_{g\perp})^2}{(1-x_p)s}$.

A. Inclusive forward particle production in pp collisions

Inclusive forward hadron production in pA/pp collisions is an important experimental observable to study dense gluonic matter in high energy scatterings [45, 51–57]. The suppression of particle yield at low transverse momentum in the forward region has been argued to be one of the “smoking gun” evidences of the saturation phenomena. Considerable experimental efforts have been made in identifying the saturation phenomenon via this observable at RHIC and LHC [58–62]. The complete NLO correction to the cross section has been worked out in Refs. [18, 19].

The numerical estimation [63] however soon reveals that the NLO cross section of the inclusive forward hadron production turns to negative at large hadron transverse momentum. By taking into account the exact kinematics near the end point, the negativity problem can be partially remedied though the cross section still becomes negative at sufficient high transverse momentum [64]. A new factorization scheme [65] using a running x'_g in the hard part calculation also offers a possible solution to this issue [66, 67]. More recently, the reorganization of the perturbation series based on the threshold resummation [68–70] is shown to be a promising approach to maintain the positivity of the cross section as well. Other attempts to fix this problem can be found in Refs. [71–75].

In this work, we adopt the subtraction scheme suggested in Ref. [65]. However, in contrast to the original proposal [65], we subtract the modified BFKL kernel presented in Eq. (9) from the hard part instead of the standard one. We show that the convergence of the perturbative series is greatly improved by absorbing the large threshold logarithm $\ln \frac{1}{1-x_p}$ arises in the NLO calculation into the kinematic constraint BFKL equation.

For the demonstration purpose, here we only consider the quark initiated channel. The LO and the NLO cross section in the hybrid approach can be organized into the following form,

$$\frac{d\sigma}{d^2p_{h\perp} dy} = \sum_f \int \frac{dz}{z^2} d\xi [x_p q_f(x_p) \mathcal{F}_{x_g}(k_\perp) + H_s + H_{ns}] D_{h/q}(z) \quad (13)$$

where the longitudinal momentum fractions carried by the incident quark and gluon are fixed

by the external kinematics $x_p = k_\perp e^y/\sqrt{s}$, $x_g = k_\perp e^{-y}/\sqrt{s}$ with k_\perp being the transverse momentum transfer to quark from the target and y being the rapidity of the produced hadron with the transverse momentum $p_{h\perp} = zk_\perp$. $q_f(x_p)$ and $D_{h/q}(z)$ are the quark PDF of the projectile proton and the collinear fragmentation function respectively. $\mathcal{F}_{x_g}(k_\perp)$ is the Fourier transform of the dipole amplitude which is related to the gluon TMD via $\mathcal{F}_{x_g}(k_\perp) = \frac{2\pi^2\alpha_s}{k_\perp^2 N_c} G(x_g, k_\perp)$.

In order to be consistent with the implementation of the BFKL evolution, the NLO correction is computed in the dilute limit following Ref. [76]. The NLO correction is separated into the singular part H_s and the non-singular part H_{ns} with the help of the identity,

$$\int_\tau^1 d\xi \frac{1+\xi^2}{1-\xi} f(\xi) \mathcal{F}_{x'_g} = \int_\tau^1 d\xi \frac{1+\xi^2}{(1-\xi)_+} f(\xi) \mathcal{F}_{x'_g} + \int_0^1 d\xi \frac{2}{1-\xi} f(1) \mathcal{F}_{x'_g} \quad (14)$$

with $f(\xi)$ being an arbitrary test function. The longitudinal momentum fraction of the mother gluon is determined as $x'_g = x_g + x_g \frac{(k_\perp - k_{g\perp})^2}{k_\perp^2} \frac{\xi}{1-\xi}$ by external kinematics [65]. Note that the "plus" prescription defined above is slightly different from the conventional one. All contributions that are free from the rapidity singularity at $\xi = 1$, i.e. the first term on the right side of the above equation are grouped into H_{ns} which reads,

$$\begin{aligned} H_{ns} = & \frac{\alpha_s}{2\pi^2} \frac{x_p}{\xi} q_f\left(\frac{x_p}{\xi}\right) \frac{1+\xi^2}{(1-\xi)_+} \int d^2k_{g\perp} \left\{ \frac{N_c}{k_\perp^2} \mathcal{F}_{x'_g}(k_{g\perp}) [1 - \theta(k_\perp - k_{g\perp}) - \theta(k_\perp - \xi k_{g\perp})] \right. \\ & + \frac{C_F}{(k_{g\perp} - k_\perp)^2} \left[\mathcal{F}_{x'_g}(k_{g\perp}) - \frac{\mu^2 \mathcal{F}_{x_g}(k_\perp)}{(k_{g\perp} - k_\perp)^2 + \mu^2} + \frac{\mathcal{F}_{\tilde{x}'_g}\left(\frac{k_\perp}{\xi} + k_{g\perp} - k_\perp\right)}{\xi^2} - \frac{1}{\xi^2} \frac{\mu^2 \mathcal{F}_{x_g/\xi}\left(\frac{k_\perp}{\xi}\right)}{(k_{g\perp} - k_\perp)^2 + \mu^2} \right] \\ & + \frac{\alpha_s}{N_c 2\pi^2} \frac{x_p}{\xi} q_f\left(\frac{x_p}{\xi}\right) \left[\frac{1+\xi^2}{(1-\xi)_+} \bar{I}_{qq}^{(1)} - \left(\frac{(1+\xi^2) \ln(1-\xi)^2}{1-\xi} \right)_+ \mathcal{F}_{x'_g}(k_\perp) \right] \\ & \left. - \frac{N_c \alpha_s}{2\pi} x_p q_f(x_p) \mathcal{F}_{x_g}(k_\perp) \int_0^1 d\xi' \frac{1+\xi'^2}{(1-\xi')_+} \ln \xi'^2 \right\} \quad (15) \end{aligned}$$

where $\tilde{x}'_g = x_g + x_g \frac{(k_\perp/\xi - k_{g\perp})^2}{k_\perp^2} \frac{\xi}{1-\xi}$. μ is the factorization scale. We emphasize again that the plus-prescription only acts on the q_f while the ξ dependencies of \mathcal{F} and $\bar{I}_{qq}^{(1)}$ are unaffected. The short hand notation $\bar{I}_{qq}^{(1)}$ stands for,

$$\begin{aligned} \bar{I}_{qq}^{(1)} = & \int d^2k_{g\perp} \left[\mathcal{F}_{x'_g}(k_{g\perp}) \frac{(k_\perp - k_{g\perp}) \cdot (k_\perp - \xi k_{g\perp})}{(k_\perp - k_{g\perp})^2 (k_\perp - \xi k_{g\perp})^2} \right. \\ & \left. - \mathcal{F}_{x'_g}(k_\perp) \left\{ \frac{(k_\perp - k_{g\perp}) \cdot (\xi k_\perp - k_{g\perp})}{(k_\perp - k_{g\perp})^2 (\xi k_\perp - k_{g\perp})^2} + \frac{k_{g\perp} \cdot (k_\perp - k_{g\perp})}{k_{g\perp}^2 (k_\perp - k_{g\perp})^2} \right\} \right]. \quad (16) \end{aligned}$$

In the above result, the collinear divergences have been removed by subtracting the NLO PDF and the NLO integrated fragmentation function in the $\overline{\text{MS}}$ scheme. When making this subtraction, we replace $1/\hat{\epsilon}$ with $\frac{1}{\hat{\epsilon}} = \int \frac{d^{2-\hat{\epsilon}}k_{g\perp}}{2\pi} \frac{\mu^{2+\hat{\epsilon}}}{k_{g\perp}^2 (k_{g\perp}^2 + \mu^2)}$ to simplify the numerical estimations.

Now we turn to discuss the singular part. We proceed by first imposing the exact kinematic cut as introduced in Ref. [64]. The upper limit of ξ integration is then modified

as,

$$\int_0^{1-\frac{(k_\perp-k_{g\perp})^2}{x_p s}} d\xi \frac{1}{1-\xi} = \ln \frac{1}{x_g} + \ln \frac{k_\perp^2}{(k_{g\perp}-k_\perp)^2} \quad (17)$$

For the virtual correction, the large logarithm $\ln \frac{1}{x_g}$ in the above formula is absorbed into the renormalized gluon TMD. We are left with the second term which should be added back to the NLO hard part. For the real correction, the large logarithm arises in the first iteration of the BFKL evolution with a rapidity veto is $\int_{x_g+\Delta x}^1 \frac{dx}{x} = \ln \frac{1}{x_g+\Delta x}$. After subtracting this small x logarithm, one ends up with,

$$\int_0^{1-\frac{(k_\perp-k_{g\perp})^2}{x_p s}} d\xi \frac{1}{1-\xi} - \int_{x_g+\Delta x}^1 \frac{dx}{x} = \ln \frac{k_\perp^2 + \frac{x_p}{1-x_p}(k_\perp - k_{g\perp})^2}{(k_\perp - k_{g\perp})^2} \quad (18)$$

which contributes to the finite part of the real correction. At large k_\perp , the above expression is reduced to $\ln \frac{1}{1-x_p}$ which would be absent if one uses the LL BFKL equation. After taking into account the the exact kinematic cut effect and subtracting the small x logarithm, one arrives at the finite part,

$$H_s = \frac{N_c \alpha_s}{\pi^2} x_p q_f(x_p) \int d^2 k_{g\perp} \left\{ \int_{1-x_g-\Delta x}^{1-\frac{(k_\perp-k_{g\perp})^2}{x_p s}} \frac{d\xi}{1-\xi} \mathcal{F}_{x'_g}(k_{g\perp}) \frac{k_{g\perp}^2}{(k_\perp - k_{g\perp})^2 k_\perp^2} \right. \\ \left. - \int_{1-x_g}^{1-\frac{(k_\perp-k_{g\perp})^2}{x_p s}} \frac{d\xi}{1-\xi} \mathcal{F}_{x'_g}(k_\perp) \frac{k_\perp^2}{(k_\perp - k_{g\perp})^2 (k_\perp^2 + (k_\perp - k_{g\perp})^2)} \right\} \quad (19)$$

One intriguing point which is worthy to be mentioned is that the above kinematic cut has to be imposed on both the real and virtual corrections simultaneously to ensure infrared finite, whereas the different treatments of kinematic constraint in Eq. 17 and Eq. 18 still lead to a infrared finite result.

Such subtraction scheme based on the NLL BFKL equation can be further refined by noticing that the probability for emitting a gluon within a given rapidity interval is not only determined by the integral $\int \frac{d\xi}{1-\xi}$, but also affected by the quark PDF $q_f(x_p/\xi)$. As well known, at large x , the quark PDF decreases very quickly when x approaches 1. To account for this effect, we introduce an effective x'_p by solving the equation,

$$\int_{x_p} d\xi \left[q_f(x_p) - q_f\left(\frac{x_p}{\xi}\right) \right] \frac{1}{1-\xi} = q_f(x_p) \ln \frac{1}{1-x'_p} \quad (20)$$

where x'_p is always larger than x_p . Only if were quark PDF an uniform distributed in the range $(x_p, 1)$, one has $x_p = x'_p$. This procedure amounts to rearrange the contribution between the fixed order corrections and the NLL BFKL kernel. To some extent, x'_p plays a role similar to a running factorization scale. In the following, we set $x'_p = 0.8$ to fix the values of Δx and x'_g for simplifying the numerical calculations.

We compute the inclusive forward hadron production in pp collisions at RHIC and LHC energies in the very forward region where the quark initiated channel dominates. The numerical results are presented in Fig. 3. One can see that the NLO result is smaller

than the LO result almost in the entire kinematic range reached at LHC, which is line with the observation made in Refs. [65–67], whereas the NLO contribution is larger than the LO one at relatively low transverse momentum for RHIC kinematics. These numerical results also confirm that the new subtraction scheme renders us to obtain a more stable NLO contribution. This is because that the part of sub-leading logarithm contribution at the NLO has been resummed by the kinematic constraint BFKL, and thus incorporated into the LO result. Moreover, the kinematic constraint BFKL appears to be a crucial ingredient for correctly describing the observed k_\perp shape. Let us close this section with a final remark. In order to fit experimental data, we adopt a somewhat unrealistic large transverse area of proton: $S_\perp = 51\text{mb}$ following Ref. [70]. Our calculation would underestimate the experimental measurements by the factor of two or three if we use the initial conditions for gluon distribution fitted to HERA data from a leading order calculation. It might be more appropriate to compute the NLO correction to the forward particle production using a fit from HERA data based on a NLO calculation [77], preferably with the kinematic constraint effect being taken into account. As it is far beyond the scope of the current work, we leave such NLO global fitting for the future study.

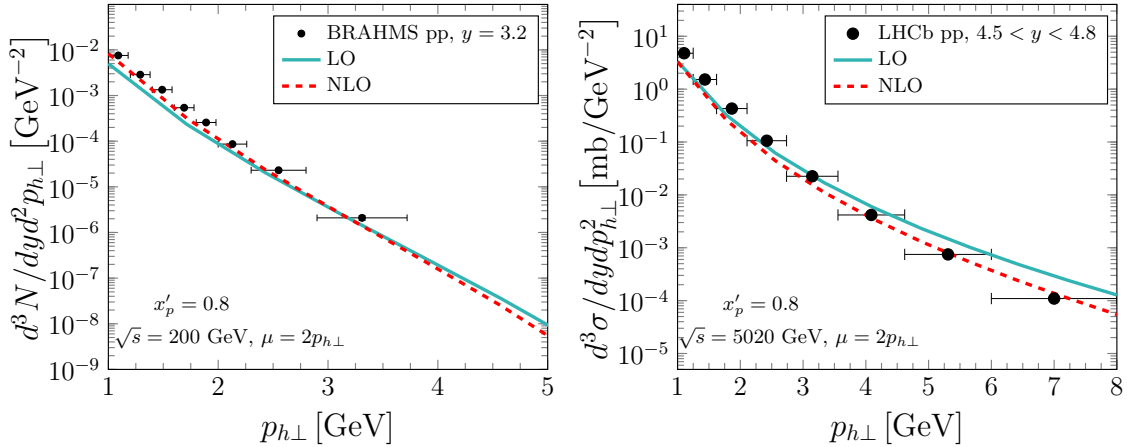


FIG. 3: Comparisons of the NLO cross sections with data from RHIC ($\sqrt{s} = 200$ GeV) and LHC ($\sqrt{s} = 5020$ GeV) in pp collisions [58, 62]. The LO results are obtained using the solution to the kinematic constraint BFKL equation.

B. Forward jet production in SIDIS

One of the golden channels for probing the saturation effect is the di-jet production in the so-called correlation limit in semi-inclusive DIS process [78–81]. Due to the relatively large invariant mass of di-jet system that is required for reconstructing jets, it is however hard to access very small x region at EIC through this observable. Moreover, the contribution to pair k_\perp broadening from the Sudakov effect could also complicate the identification of the saturation effects. Alternatively, the saturation effect can be observed in the semi-inclusive production of a single hadron(or jet) as well [82]. In particular, the sensitivity of this process to gluon saturation has been argued to be enhanced in the threshold region where the produced hadron(or jet) carries a large longitudinal momentum fraction($z \approx 1$) of the

incoming virtual photon [83]. This is precisely the region where the kinematic constraint discussed above could play an important role.

In the leading order calculation of the SIDIS process, the minus component of the exchanged gluons momenta is strictly set to be zero. However, in reality, the exchanged gluon carries a nonvanishing minus component of the light cone momentum acquired from the radiated gluons in the cascade due to the recoil effect. Though this is formally a next leading power contribution, it can be very important in the threshold region as discussed in the previous section. To account for this effect, we explicitly keep the finite minus component of the exchanged gluons in the following analysis, and denote the longitudinal momentum fractions of virtual photon shared by the produced jet, unobserved quark/anti-quark and the radiated gluon as z , z_1 and z_2 which satisfy the relation $z + z_1 + z_2 = 1$ and $z_1 \sim z_2 \ll z \sim 1$.

We only consider transverse photon production of jet, as the longitudinal SIDIS cross section is suppressed by the factor z_1 in the threshold region. At the leading order, the transverse SIDIS cross section in the small x formalism can be cast into a fairly compact form [83],

$$\frac{d\sigma}{dzd^2k_\perp} = 2S_\perp N_c \frac{\alpha_{em}}{\pi} e_f^2 [z^2 + (1-z)^2] \mathcal{J}_T \quad (21)$$

with

$$\mathcal{J}_T = \int \frac{d^2r_\perp}{(2\pi)^2} e^{-ik_\perp \cdot r_\perp} \left\{ \frac{ik_\perp \cdot r_\perp}{\bar{Q}|r_\perp|} \frac{\bar{Q}^2 K_1(\bar{Q}|r_\perp|)}{k_\perp^2 + \bar{Q}^2} - \frac{1}{2} \left[K_0(\bar{Q}|r_\perp|) - \frac{\bar{Q}|r_\perp|}{2} K_1(\bar{Q}|r_\perp|) \right] \right\} \mathcal{F}_{x_g}(r_\perp) \quad (22)$$

where k_\perp is the produced jet transverse momentum. K_0 and K_1 are the modified Bessel functions. $\mathcal{F}_{x_g}(r_\perp)$ is the Fourier transform of $\mathcal{F}_{x_g}(k_\perp)$. \bar{Q} is defined as $\bar{Q}^2 = zz_1 Q^2$ with Q being the incoming photon's virtuality. The longitudinal momentum fraction of the probed gluons are determined by the external kinematics according to [83],

$$x_g = \frac{1}{2P \cdot q} \left(\frac{k_\perp^2}{z} + \frac{\max(\bar{Q}^2, Q_s^2)}{z_1} + Q^2 \right) \quad (23)$$

The above formula also can be easily converted into the momentum space expression [84].

Since the BFKL description only can apply in the dilute limit, we restrict ourself to study the k_\perp spectrum at large transverse momentum. The numerical results for the quantity $k_\perp^2 \mathcal{J}_T$ are presented as the function of k_\perp in Fig.4. At EIC energy, the kinematics are chosen to be $2P \cdot q = 10^4 \text{GeV}^2$ and $Q^2 = 10 \text{GeV}^2$. The predication is made for the configuration $z = 0.8$, $z_1 = 0.1$ and $z_2 = 0.1$. The numerical results are presented in Fig. 4. At intermediate transverse momentum, the cross section is suppressed by roughly 20% due to the kinematic constraint effect. At high transverse momentum where x_g approaches 0.01, the contribution mainly comes from the initial gluon distribution. Therefore, the results that are from the standard BFKL evolution and the kinematic constraint version converge at high transverse momentum.

IV. SUMMARY

In this work, we have introduced a BFKL equation with the kinematic constraint near threshold region, which approximately ensures the longitudinal momentum conservation.

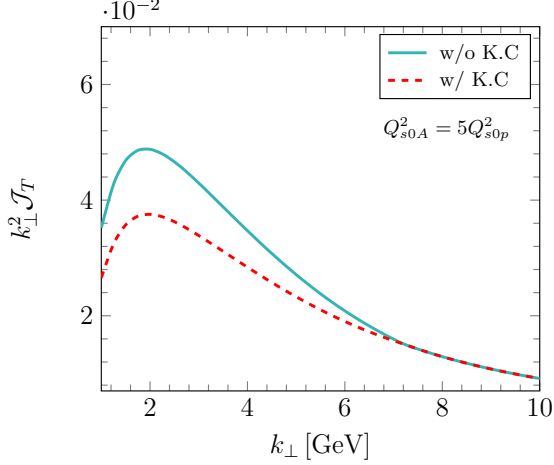


FIG. 4: The comparisons of the transverse inelastic cross section multiplied by k_{\perp}^2 with and without the kinematic constraint.

Due to the rather limited phase space available for real radiation in the threshold region, such NLL BFKL generally slow down small x evolution in particular at high transverse momentum. It differs from the conventional kinematic constraint BFKL equation results from requirement that the offshellness of exchanged gluon is dominated by transverse components. We show that the subtraction of the kinematic constraint NLL BFKL kernel from the unsubtracted hard part can lead to a more stable NLO contribution to the inclusive forward hadron production in pp collisions at high transverse momentum. We carry out the detailed numerical studies of this observable for RHIC and LHC energies and found the good agreement with the experimental data. We investigated the impact of such NLL BFKL evolution on the forward jet production in SIDIS process as well.

There are a number of directions in which the present work can be extended. First, a complete and sophisticated phenomenological analysis of the observable would require us to take into account saturation effect using a running coupling BK equation with the same external kinematic constraint. However, we do not expect that such NLL contribution arises from the kinematic effect plays an important role at low transverse momentum as it mainly modifies high k_{\perp} tail behavior. Second, one may notice that the longitudinal momentum conservation (along the projectile direction) is only approximately kept in our treatment. To impose the longitudinal momentum conservation locally in the each step of the evolution, it is highly desirable to develop a Monte Carlo event generator based on the NLL BK equation. Lastly, it would be also interesting to apply our approach to other processes, such as forward di-jet production in pA or eA collisions.

Acknowledgments

We thank Shu-yi Wei for helpful discussions. Jian Zhou has been supported by the National Natural Science Foundations of China under Grant No. 12175118. Hao-yu Liu has

been supported by the China Postdoctoral Science Foundation under Grant No. 212400211.

-
- [1] E. A. Kuraev, L. N. Lipatov, and V. S. Fadin, *Sov. Phys. JETP* **45**, 199 (1977).
 - [2] I. I. Balitsky and L. N. Lipatov, *Sov. J. Nucl. Phys.* **28**, 822 (1978).
 - [3] J. Jalilian-Marian, A. Kovner, A. Leonidov, and H. Weigert, *Phys. Rev. D* **59**, 014014 (1998), hep-ph/9706377.
 - [4] J. Jalilian-Marian, A. Kovner, A. Leonidov, and H. Weigert, *Nucl. Phys. B* **504**, 415 (1997), hep-ph/9701284.
 - [5] J. Jalilian-Marian, A. Kovner, L. D. McLerran, and H. Weigert, *Phys. Rev. D* **55**, 5414 (1997), hep-ph/9606337.
 - [6] E. Iancu and L. D. McLerran, *Phys. Lett. B* **510**, 145 (2001), hep-ph/0103032.
 - [7] I. Balitsky, *Nucl. Phys. B* **463**, 99 (1996), hep-ph/9509348.
 - [8] Y. V. Kovchegov, *Phys. Rev. D* **60**, 034008 (1999), hep-ph/9901281.
 - [9] V. S. Fadin and L. N. Lipatov, *Nucl. Phys. B* **477**, 767 (1996), hep-ph/9602287.
 - [10] M. Ciafaloni and G. Camici, *Phys. Lett. B* **430**, 349 (1998), hep-ph/9803389.
 - [11] I. Balitsky and G. A. Chirilli, *Phys. Rev. D* **77**, 014019 (2008), 0710.4330.
 - [12] I. Balitsky and G. A. Chirilli, *Phys. Rev. D* **88**, 111501 (2013), 1309.7644.
 - [13] A. H. Mueller, B.-W. Xiao, and F. Yuan, *Phys. Rev. Lett.* **110**, 082301 (2013), 1210.5792.
 - [14] A. H. Mueller, B.-W. Xiao, and F. Yuan, *Phys. Rev. D* **88**, 114010 (2013), 1308.2993.
 - [15] J. Zhou, *JHEP* **06**, 151 (2016), 1603.07426.
 - [16] B.-W. Xiao, F. Yuan, and J. Zhou, *Nucl. Phys. B* **921**, 104 (2017), 1703.06163.
 - [17] J. Zhou, *Phys. Rev. D* **99**, 054026 (2019), 1807.00506.
 - [18] G. A. Chirilli, B.-W. Xiao, and F. Yuan, *Phys. Rev. Lett.* **108**, 122301 (2012), 1112.1061.
 - [19] G. A. Chirilli, B.-W. Xiao, and F. Yuan, *Phys. Rev. D* **86**, 054005 (2012), 1203.6139.
 - [20] I. Balitsky and G. A. Chirilli, *Phys. Rev. D* **87**, 014013 (2013), 1207.3844.
 - [21] G. Beuf, *Phys. Rev. D* **85**, 034039 (2012), 1112.4501.
 - [22] R. Boussarie, A. V. Grabovsky, L. Szymanowski, and S. Wallon, *JHEP* **11**, 149 (2016), 1606.00419.
 - [23] R. Boussarie, A. V. Grabovsky, D. Y. Ivanov, L. Szymanowski, and S. Wallon, *Phys. Rev. Lett.* **119**, 072002 (2017), 1612.08026.
 - [24] G. Beuf, *Phys. Rev. D* **96**, 074033 (2017), 1708.06557.
 - [25] H. Hänninen, T. Lappi, and R. Paatelainen, *Annals Phys.* **393**, 358 (2018), 1711.08207.
 - [26] K. Roy and R. Venugopalan, *JHEP* **05**, 013 (2018), 1802.09550.
 - [27] K. Roy and R. Venugopalan, *Phys. Rev. D* **101**, 034028 (2020), 1911.04530.
 - [28] R. Boussarie, A. V. Grabovsky, L. Szymanowski, and S. Wallon, *Phys. Rev. D* **100**, 074020 (2019), 1905.07371.
 - [29] H. Mäntysaari and J. Penttala, *Phys. Lett. B* **823**, 136723 (2021), 2104.02349.
 - [30] E. Iancu and Y. Mulian, *JHEP* **03**, 005 (2021), 2009.11930.
 - [31] G. Beuf, T. Lappi, and R. Paatelainen, *Phys. Rev. D* **104**, 056032 (2021), 2103.14549.
 - [32] P. Caucal, F. Salazar, and R. Venugopalan (2021), 2108.06347.
 - [33] M. Ciafaloni, *Nucl. Phys. B* **296**, 49 (1988).
 - [34] S. Catani, F. Fiorani, and G. Marchesini, *Phys. Lett. B* **234**, 339 (1990).
 - [35] B. Andersson, G. Gustafson, and J. Samuelsson, *Nucl. Phys. B* **467**, 443 (1996).
 - [36] J. Kwiecinski, A. D. Martin, and P. J. Sutton, *Z. Phys. C* **71**, 585 (1996), hep-ph/9602320.

- [37] J. Kwiecinski, A. D. Martin, and A. M. Stasto, Phys. Rev. D **56**, 3991 (1997), hep-ph/9703445.
- [38] J. R. Andersen et al. (Small x), Eur. Phys. J. C **48**, 53 (2006), hep-ph/0604189.
- [39] M. Deak, K. Kutak, W. Li, and A. M. Stasto, Eur. Phys. J. C **79**, 647 (2019), 1906.09062.
- [40] E. Iancu, J. D. Madrigal, A. H. Mueller, G. Soyez, and D. N. Triantafyllopoulos, Phys. Lett. B **744**, 293 (2015), 1502.05642.
- [41] B. Ducloué, E. Iancu, A. H. Mueller, G. Soyez, and D. N. Triantafyllopoulos, JHEP **04**, 081 (2019), 1902.06637.
- [42] D.-X. Zheng and J. Zhou, JHEP **11**, 177 (2019), 1906.06825.
- [43] W.-C. Xiang, M.-L. Wang, Y.-B. Cai, and D.-C. Zhou, Chin. Phys. C **45**, 014103 (2021), 2008.04235.
- [44] W. Xiang, Y. Cai, M. Wang, and D. Zhou, Phys. Rev. D **104**, 016018 (2021), 2102.03789.
- [45] A. Dumitru and J. Jalilian-Marian, Phys. Lett. B **547**, 15 (2002), hep-ph/0111357.
- [46] E. Iancu, J. D. Madrigal, A. H. Mueller, G. Soyez, and D. N. Triantafyllopoulos, Phys. Lett. B **750**, 643 (2015), 1507.03651.
- [47] T. Lappi and H. Mäntysaari, Phys. Rev. D **93**, 094004 (2016), 1601.06598.
- [48] Y. Hatta and E. Iancu, JHEP **08**, 083 (2016), 1606.03269.
- [49] E. Avsar, A. M. Stasto, D. N. Triantafyllopoulos, and D. Zaslavsky, JHEP **10**, 138 (2011), 1107.1252.
- [50] Y. V. Kovchegov and H. Weigert, Nucl. Phys. A **789**, 260 (2007), hep-ph/0612071.
- [51] D. Kharzeev, Y. V. Kovchegov, and K. Tuchin, Phys. Rev. D **68**, 094013 (2003), hep-ph/0307037.
- [52] J. P. Blaizot, F. Gelis, and R. Venugopalan, Nucl. Phys. A **743**, 13 (2004), hep-ph/0402256.
- [53] J. P. Blaizot, F. Gelis, and R. Venugopalan, Nucl. Phys. A **743**, 57 (2004), hep-ph/0402257.
- [54] A. Dumitru, A. Hayashigaki, and J. Jalilian-Marian, Nucl. Phys. A **765**, 464 (2006), hep-ph/0506308.
- [55] J. L. Albacete and C. Marquet, Phys. Lett. B **687**, 174 (2010), 1001.1378.
- [56] V. Guzey, M. Strikman, and W. Vogelsang, Phys. Lett. B **603**, 173 (2004), hep-ph/0407201.
- [57] T. Altinoluk and A. Kovner, Phys. Rev. D **83**, 105004 (2011), 1102.5327.
- [58] I. Arsene et al. (BRAHMS), Phys. Rev. Lett. **93**, 242303 (2004), nucl-ex/0403005.
- [59] J. Adams et al. (STAR), Phys. Rev. Lett. **97**, 152302 (2006), nucl-ex/0602011.
- [60] S. Acharya et al. (ALICE), Eur. Phys. J. C **78**, 624 (2018), 1801.07051.
- [61] G. Aad et al. (ATLAS), Phys. Lett. B **763**, 313 (2016), 1605.06436.
- [62] R. Aaij et al. (LHCb) (2021), 2108.13115.
- [63] A. M. Stasto, B.-W. Xiao, and D. Zaslavsky, Phys. Rev. Lett. **112**, 012302 (2014), 1307.4057.
- [64] K. Watanabe, B.-W. Xiao, F. Yuan, and D. Zaslavsky, Phys. Rev. D **92**, 034026 (2015), 1505.05183.
- [65] E. Iancu, A. H. Mueller, and D. N. Triantafyllopoulos, JHEP **12**, 041 (2016), 1608.05293.
- [66] B. Ducloué, T. Lappi, and Y. Zhu, Phys. Rev. D **95**, 114007 (2017), 1703.04962.
- [67] B. Ducloué, E. Iancu, T. Lappi, A. H. Mueller, G. Soyez, D. N. Triantafyllopoulos, and Y. Zhu, Nucl. Phys. A **982**, 271 (2019), 1807.04971.
- [68] B.-W. Xiao and F. Yuan, Phys. Lett. B **788**, 261 (2019), 1806.03522.
- [69] H.-Y. Liu, Z.-B. Kang, and X. Liu, Phys. Rev. D **102**, 051502 (2020), 2004.11990.
- [70] Y. Shi, L. Wang, S.-Y. Wei, and B.-W. Xiao (2021), 2112.06975.
- [71] A. M. Stasto, B.-W. Xiao, F. Yuan, and D. Zaslavsky, Phys. Rev. D **90**, 014047 (2014), 1405.6311.
- [72] T. Altinoluk, N. Armesto, G. Beuf, A. Kovner, and M. Lublinsky, Phys. Rev. D **91**, 094016

- (2015), 1411.2869.
- [73] Z.-B. Kang, I. Vitev, and H. Xing, Phys. Rev. Lett. **113**, 062002 (2014), 1403.5221.
 - [74] B. Ducloué, T. Lappi, and Y. Zhu, Phys. Rev. D **93**, 114016 (2016), 1604.00225.
 - [75] B.-W. Xiao and F. Yuan (2014), 1407.6314.
 - [76] K. Watanabe and B.-W. Xiao, Phys. Rev. D **94**, 094046 (2016), 1607.04726.
 - [77] G. Beuf, H. Hänninen, T. Lappi, and H. Mäntysaari, Phys. Rev. D **102**, 074028 (2020), 2007.01645.
 - [78] A. Kovner and U. A. Wiedemann, Phys. Rev. D **64**, 114002 (2001), hep-ph/0106240.
 - [79] F. Gelis and J. Jalilian-Marian, Phys. Rev. D **67**, 074019 (2003), hep-ph/0211363.
 - [80] F. Dominguez, C. Marquet, B.-W. Xiao, and F. Yuan, Phys. Rev. D **83**, 105005 (2011), 1101.0715.
 - [81] A. Metz and J. Zhou, Phys. Rev. D **84**, 051503 (2011), 1105.1991.
 - [82] A. H. Mueller, Nucl. Phys. B **558**, 285 (1999), hep-ph/9904404.
 - [83] E. Iancu, A. H. Mueller, D. N. Triantafyllopoulos, and S. Y. Wei, JHEP **07**, 196 (2021), 2012.08562.
 - [84] H. Dong, D.-X. Zheng, and J. Zhou, Phys. Lett. B **788**, 401 (2019), 1805.09479.